frontiers | Frontiers in Materials

TYPE Original Research
PUBLISHED 26 January 2026
DOI 10.3389/fmats.2026.1759190

OPEN ACCESS

EDITED BY
Pengfei Liu,
RWTH Aachen University, Germany

REVIEWED BY
Chaoliang Fu,
RWTH Aachen University, Germany
Hanyu Zhang,
Liverpool John Moores University, United Kingdom
Germain Djinsi Vaïmata,
University of Maroua, Cameroon

*CORRESPONDENCE
Rui Wu,
r.wu-2@tudelft.nl

RECEIVED 02 December 2025
REVISED 08 January 2026
ACCEPTED 12 January 2026
PUBLISHED 26 January 2026

CITATION
Zhang G, Cao F, Li T, Sun C, Yao L, Chang Y, Su W, Chen H, Guo W, Wu R and Ma B (2026) Experimental study and mechanism analysis on improving the workability of metakaolin-based geopolymers using superplasticizer.
Front. Mater. 13:1759190.
doi: 10.3389/fmats.2026.1759190

Experimental study and mechanism analysis on improving the workability of metakaolin-based geopolymers using superplasticizer

Genhe Zhang[1,2], Feng Cao[2], Taotao Li[2], Chao Sun[2], Linhao Yao[1], Yongqi Chang[1], Wenbin Su[1], Hao Chen[1], Wei Guo[1], Rui Wu[3]* and Biao Ma[1]

[1]School of Highway, Chang'an University, Xi'an, Shaanxi, China, [2]The 7th Engineering Co., Ltd. of CCCC Second Highway Engineering Bureau, Nanning, Guangxi, China, [3]Faculty of Civil Engineering and Geosciences, Delft University of Technology, Delft, Netherlands

Metakaolin-based geopolymer is considered a potential alternative to traditional cement materials; however, its fresh paste typically suffers from high viscosity and poor workability. To evaluate the effect of superplasticizers, this study first optimized the basic mix proportions of alkali-activated metakaolin geopolymer through orthogonal testing. The influences of five superplasticizers—melamine, sodium lignosulfonate, naphthalene-based, polycarboxylate, and KH-550 at varying dosages were then examined in terms of flowability and compressive strength. The mechanisms of superplasticizer action were further investigated by means of physical stability assessment, Fourier-transform infrared spectroscopy (FTIR), surface tension, and zeta potential testing. The results indicate that the optimal mix design for the metakaolin-based geopolymer is achieved with a silicate modulus of 0.9, a liquid-to-solid ratio of 0.75, and a silica fume content of 15%, leading to a 28-day compressive strength of 58.8 MPa and a flow diameter of 132 mm. Compared with other superplasticizer, sodium lignosulfonate exhibited superior water-reducing efficiency and stability, while its adverse effect on compressive strength was acceptable. Balancing workability and strength requirements, the optimal dosage was determined to be 1.5%. Mechanism analysis further revealed that superplasticizer can enhance electrostatic repulsion between particles, thereby improving the flowability of metakaolin-based geopolymers. This research provides a viable pathway for preparing metakaolin-based geopolymers with superior mechanical properties and workability.

KEYWORDS

geopolymer, mechanical property, mechanism, metakaolin, mobility, superplasticizer

1 Introduction

In response to global climate change and resource shortages, developing green and low-carbon building materials has become a critical direction for upgrading the construction industry (Hu et al., 2025a; Li et al., 2025; Si et al., 2024; Hu et al., 2025b). Geopolymers are amorphous three-dimensional network gels. Their structure is formed

through the crosslinking of silicon–oxygen tetrahedra $(SiO_4)^{4-}$ and aluminum–oxygen tetrahedra $(AlO_4)^{5-}$, which share oxygen atoms at their vertices. Their raw materials typically include fly ash, granulated blast-furnace slag, and metakaolin, together with alkaline or acidic activators (Li et al., 2018; Aupoil et al., 2019; Ge et al., 2022). Compared with ordinary Portland cement, geopolymers not only exhibit excellent mechanical, acid, heat and fire resistance properties (Asghar et al., 2023), they also consume only 1/6 to 1/4 of the energy required for cement production, making them promising low-carbon binders (Shi et al., 2019).

The existing research mainly focuses on fly ash-based and slag-based polymer systems (Nath and Sarker, 2014; Aziz et al., 2020). However, fly ash has low reactivity and often requires high temperature curing to obtain adequate early age strength. Slag-based systems, in contrast, face practical challenges such as short setting times, high shrinkage, and an increased risk of cracking (Shi et al., 2025a; Singh et al., 2016). Metakaolin offers advantages such as low impurity content, uniform composition, room-temperature preparation, and high product stability (Kou et al., 2011). Nevertheless, metakaolin-based geopolymers typically exhibit poor workability, including high viscosity and low flowability, which limits their engineering application (Keskin-Topan et al., 2024).

To address these limitations, one research pathway focuses on optimizing mix proportions and activation conditions (Hu et al., 2025c; Si et al., 2026). Huang and Wang (Huang and Wang, 2024) achieved workability comparable to cement paste by adjusting the liquid-to-solid ratio while maintaining compressive strength. Liu et al.(Liu et al., 2023) found that increasing the silicate modulus from 1.1 to 1.5 significantly improved flowability, whereas exceeding 1.5 resulted in reduced fluidity. Zhong et al. (Zhong et al., 2023) showed that increasing the silicate modulus decreased the yield stress and plastic viscosity of metakaolin-slag geopolymer, thus obtaining better fluidity. The second pathway involves the use of high-performance superplasticizers (Shi et al., 2025b). The main types of superplasticizer include polycarboxylates, melamine, naphthalene-based additives, sodium lignosulfonate, and silane coupling agents (Lu et al., 2021). However, their effectiveness varies across alkali-activated systems. Palacios and Puertas (2005) found that only naphthalene-based superplasticizers improved the workability of alkali-activated slag systems, while others tended to hydrolyze. Rakngan et al. (2018) pointed out that although naphthalene superplasticizer can improve the working performance of alkali-activated fly ash paste, they have adverse effects on its strength after hardening. Ye et al. (2016) demonstrated that adding 0.5 wt% sodium lignosulfonate enhanced the strength of red-mud-based geopolymers by lowering the water-to-solid ratio. Despite these findings, the chemical stability, interfacial behavior, and water-reduction mechanisms of superplasticizers in highly alkaline metakaolin systems remain insufficiently understood (Li et al., 2024; Shi et al., 2025b).

In this study, orthogonal experiments were first conducted to optimize the mix design of metakaolin-based geopolymers by balancing workability and compressive strength. Secondly, the effects of five superplasticizers, specifically melamine, sodium lignosulfonate, naphthalene-based superplasticizer, polycarboxylate superplasticizer, and the KH 550 silane coupling agent, on the workability of fresh paste were systematically evaluated using initial flowability and bleeding volume as indicators. Based on these results, the most suitable superplasticizer was identified. The influence of varying dosages of the optimal superplasticizer on the time-dependent loss of paste flowability and on compressive strength was examined to determine its optimal dosage. Finally, through physical stability tests, Fourier-transform infrared spectroscopy (FTIR), surface tension tests, and paste zeta potential analysis, the action mechanisms of various superplasticizer were investigated.

2 Raw materials and test methods

2.1 Raw material

Metakaolin was selected as geopolymer precursor material and silica fume (SiO_2 > 90%) was used as modifier; both materials were purchased from Chenyi Refractory Abrasives. The chemical composition and phase composition were determined by X-ray fluorescence and X-ray diffraction, respectively, as shown in Table 1 and Figure 1. Alkali activators used in the experiment are sodium silicate solution (8.2 wt% Na_2O, 26 wt% SiO_2, 65.8 wt% H_2O) and sodium hydroxide solution (purity 99%). The modulus of sodium silicate can be adjusted by adding NaOH.

Superplasticizer, as important functional components of geopolymers, play a crucial role in improving paste workability (Johnson et al., 2023). Melamine, sodium lignosulfonate, naphthalene superplasticizer, polycarboxylic acid superplasticizer and KH550 silane coupling agent were selected as superplasticizers in this study.

2.2 Geopolymer preparation

2.2.1 Preparation of alkali activator

Add sodium silicate and deionized water into a beaker, stir well with a glass rod, then add accurately predesigned amount of sodium hydroxide, stir until the particles are completely dissolved, cover with plastic wrap to prevent moisture volatilization. Make the activator stand by for about 4 h, until the solution cools to room temperature and becomes clear before use. For every 100 g of sodium silicate solution prepared into an alkali activator of modulus n, the mass x of sodium hydroxide required is determined by Equation 1.

$$n = \frac{26/60}{8.2/62 + x/80} = \frac{0.433}{0.132 + x/80} \quad (1)$$

2.2.2 Geopolymer sample preparation

The alkali activator and precursor materials were mixed according to the designed proportions. The mixture was first stirred at a low speed for 1–3 min to ensure uniform wetting, followed by high-speed mixing for an additional 2–5 min to achieve full homogenization. Immediately after mixing, the fresh paste was injected into the test molds. Compressive strength specimens were prepared using silicone molds with dimensions of 20 mm × 20 mm × 20 mm, with three replicates for each group. The paste was manually compacted and then placed on a vibrating table for 30–60 s to remove entrapped air, followed by surface leveling. After casting,

TABLE 1 Content of metakaolin and silica fume (WT%).

Type	Al_2O_3	SiO_2	Fe_2O_3	TiO_2	CaO	K_2O	MgO	Na_2O	SO_3	Others
Metakaolin	47.55	46.32	2.94	1.78	0.52	0.28	0.2	—	—	0.4
Silica fume	0.7	91.06	3.19	—	0.66	0.95	1.21	1.18	0.65	0.5

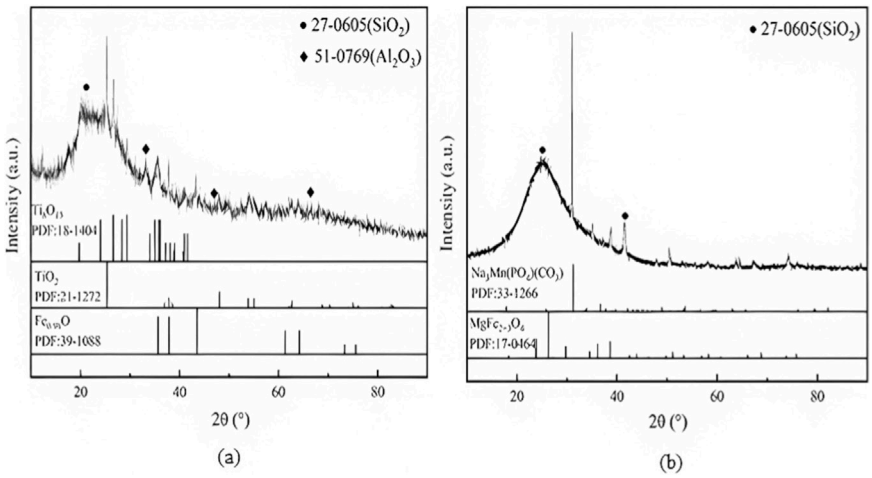

FIGURE 1
XRD spectra of metakaolin and silica fume: **(a)** Metakaolin; **(b)** Silica fume.

the specimens were covered with plastic film and cured at 25 °C for 24 h. They were then demolded and transferred to standard curing conditions (25 °C ± 2 °C and RH ≥ 95%.) until the designated testing ages. Compressive strength tests were performed at the specified curing times.

2.3 Test methods

2.3.1 Orthogonal test

To evaluate the influence of metakaolin based polymer composition on compressive strength and fluidity, orthogonal test was designed. It studied the combination of several factors at different levels to determine the optimum ratio conditions. In the orthogonal test, the modulus of sodium silicate (factor A), silica fume content (factor B) and liquid-solid ratio (factor C) were selected. Combined with the previous research results from the research group (Wang et al., 2025; Ma et al., 2020), the levels of each factor are shown in Table 2.

The $L^9(33)$ orthogonal experimental design with 3 factors and 3 levels was employed. The experimental schemes are shown in Table 3.

To investigate the influence of different factors on compressive strength of metakaolin based polymer, this study calculated the heat collection efficiency and maximum cooling value ki for each factor at level i, as well as the range R between all ki of the same factor (with i values for factors A, B, and C being 1 to 3). The specific calculation methods are shown in Equations 2, 3.

$$k_i = \frac{\sum v(i)}{n} \tag{2}$$

$$R = \max\{k_1, k_2, k_3\} - \min\{k_1, k_2, k_3\} \tag{3}$$

where k_i represents the compressive strength when a factor is at level i; R value reflects the degree of influence of the factor on compressive strength. The larger the R value, the more significant the influence on compressive strength of geopolymer.

2.3.2 Compressive property

Compressive strength tests of the metakaolin-based geopolymer at the ages of 3, 7, and 28 days were conducted using an electrohydraulic servo press with a capacity of 300 kN and a loading rate of 2 mm/min. The testing procedure followed the requirements of ASTM C109.

2.3.3 Fluidity test

To evaluate the working performance of metakaolin geopolymer paste, the fluidity of metakaolin geopolymer was measured according to the cement paste fluidity measurement method specified in the standard GB/T8077-2012 "Test Method for Homogeneity of Concrete Superplasticizer."

2.3.4 Bleeding volume test

To study the influence of superplasticizer on bleeding volume of geopolymer slurry, reference experiments were carried out with high and low additive contents. In high dosage group, melamine,

TABLE 2 The factors and levels in the orthogonal experiment.

Level	Factors		
	A (silicate modulus)	B (silica fume content, %)	C (liquid-solid ratio)
1	0.8	15	0.75
2	0.9	20	0.85
3	1.0	25	0.95

TABLE 3 Orthogonal experiment table used in this study.

Combination	Factor A	Factor B	Factor C
1	0.8	15	0.95
2	0.8	20	0.85
3	0.8	25	0.75
4	0.9	15	0.75
5	0.9	20	0.95
6	0.9	25	0.85
7	1.0	15	0.85
8	1.0	20	0.75
9	1.0	25	0.95

sodium lignosulfonate and naphthalene superplasticizer were 2.5%, polycarboxylic acid 1%, silane coupling agent KH550 0.2 mL, while in low dosage group, melamine, sodium lignosulfonate and naphthalene superplasticizer were 1%, polycarboxylic acid 0.5%, silane coupling agent 0.1 mL. Weigh 20 g metakaolin and the corresponding amount of superplasticizer into a measuring cylinder, stir evenly with a glass rod, add sodium silicate solution with modulus of 0.9 and mix well to make a constant volume of 100 mL. The bleeding volume is the supernatant volume of the slurry, record every 20 min.

2.3.5 Physical stability

Mix 0.1 g additive with 8 mL sodium silicate solution with different modulus (0.8, 1.4, 2.0), observe the stability of additive in appearance, such as agglomeration, separation, or color change. According to the principle of maximum wavelength selection, the optimum determination wavelengths of melamine, sodium lignosulfonate, naphthalene series, polycarboxylic acid and KH550 were 236 nm, 428 nm, 427 nm, 272 nm and 301 nm respectively; Secondly, prepare several additive solutions with known concentrations and test their absorbance at corresponding detection wavelengths; mix 0.1 g of additive with 8 mL of sodium silicate solution with different moduli (0.8 and 1.4), test the absorbance of supernatant with ultraviolet visible spectrophotometer and substitute it into the standard curve fitting equation to obtain the actual concentration C'. Calculate the insolubility η as per Equation 4.

$$\eta = \frac{C_0 - C'}{C_0} \times 100\% \tag{4}$$

2.3.6 Fourier transform infrared spectroscopy

Fourier transform infrared spectroscopy (FT-IR) was employed to analyze the structural change of superplasticizers and characterize the chemical stability of different superplasticizers. The measurement range was 4,000 to 400 cm^{-1} with the resolution of 4 cm^{-1} and 32 scans (Hu et al., 2024).

2.3.7 Surface tension test

To study the effect of superplasticizer on the surface tension of slurry, a sodium silicate solution with modulus of 0.9 was selected and mixed according to the proportion of 0.1 g additive per 8 mL sodium silicate solution. After mixing, the solution was allowed to stand for 24 h, and then the supernatant was processed by centrifuge. The surface tension was measured by ADVANCEKRUSS (Germany) instrument. Water solution was selected as the reference.

2.3.8 Zeta potential measurements

The zeta potential of metakaolin suspensions was measured to evaluate the influence of different superplasticizers under varying sodium silicate moduli. In the preparation process, the alkali activator, metakaolin, and the designated additive were successively added into a beaker and stirred magnetically for 2 min to ensure uniform dispersion. Subsequently, a 2 mL aliquot of the suspension was immediately extracted and transferred into the sample cell for zeta potential measurement. All tests were conducted at room temperature to minimize environmental interference, and each measurement was repeated three times to ensure accuracy and reproducibility.

3 Results and discussion

3.1 Analysis of orthogonal test results

Table 4 shows the orthogonal test results of compressive strength and fluidity of metakaolin-based polymer.

To quantitatively evaluate the significance of different factors on compressive strength, this study further carried out range analysis and analysis of variance (ANOVA), and the results

10.3389/fmats.2026.1759190

TABLE 4 Results of orthogonal test for compressive strength of metakaolin-based polymer.

Combination	Silicate modulus	Silica fume content (%)	Liquid-solid ratio	Compressive strength (MPa)			Fluidity (mm)
				3d	7d	28d	
1	1.0	15	0.95	4.2	5.3	6.7	136
2	1.0	20	0.85	10.0	18.8	24.4	133
3	1.0	25	0.75	21.0	37.2	43	128
4	0.9	15	0.75	39.7	54.7	58.8	132
5	0.9	20	0.95	12.8	13.2	15.6	134
6	0.9	25	0.85	31.2	35.3	37.5	129
7	0.8	15	0.85	21.2	29.3	36.6	117
8	0.8	20	0.75	25.5	40.1	48.0	113
9	0.8	25	0.95	12.5	14.0	17.0	122

are shown in Table 5. When the p value is less than 0.05, the influence of this factor on compressive strength index is statistically significant.

3.1.1 Compressive strength

Because the mechanical performance of geopolymers is highly sensitive to mix-design variables, this subsection compares the influence of silicate modulus, silica fume content, and liquid-to-solid ratio on compressive strength and strength development. The objective is to identify the formulation that maximizes early and long-term performance. It can be seen from Table 4 that the combination of A2B1C1 (i.e., silicate modulus 0.9, silica fume content 15%, liquid-solid ratio 0.75) showed the highest compressive strength at all ages, which was significantly better than other ratio combinations. Combined with the range and variance analysis results in Table 5, it can be seen that the liquid-solid ratio (C) and the silicate modulus (A) have significant effects on the strength development ($p < 0.05$), where the liquid-solid ratio is the dominant factor, the optimal level is C1 (0.75), and the optimal level of sodium silicate modulus is A2 (0.9). In contrast, the effect of silica fume content (B) is not significant, but the strength performance is better at B1 (15%). Therefore, A2B1C1 is not only verified statistically, but also shows mechanical advantage in measured properties. In addition, although the fluidity (132 mm) of the combination is lower than that of the higher liquid-solid ratio group, it is still in an acceptable range and can meet the construction requirements.

To further analyze the increasing trend of compressive strength of geopolymer, the results of nine groups of specimens at different ages are shown in Figure 2. The compressive strength of metakaolin geopolymer at 3d age can reach 40%~70% of 28d strength, and the compressive strength at 7d can generally reach more than 80% of 28d compressive strength, which has significant early strength. When the strength level is lower (<20 MPa), the compressive strength of 3 days is similar with that of 28 days. When the strength level is higher (>20 MPa), the compressive strength of 7 days is obviously higher than that of 3 days, but the increase of 28 days is limited, which indicates that the strength of metakaolin-based polymer mainly develops rapidly in the early stage and tends to be stable.

As shown in Figure 2, the A2B1C1 mixture exhibited the highest compressive strength and growth rate among all specimens. Its strength reached nearly 40 MPa at 3 days, increased to about 55 MPa at 7 days, and further rose to nearly 60 MPa at 28 days, showing a typical pattern of rapid early development followed by stabilization at later ages. This superior performance is attributed to the optimized silicate modulus (0.9), silica fume content (15%), and liquid-to-solid ratio (0.75), which promote aluminosilicate dissolution and dense gel formation. Similar results were reported by Hattaf et al. (2021) and Gao et al. (2014), who found that a moderate silicate modulus facilitates early geopolymerization and improves structural compactness, leading to enhanced strength and long-term stability.

3.1.2 Fluidity

It can be seen from Table 5 that, in terms of fluidity, the effect of sodium silicate modulus (A) has statistical significance at the significance level of 0.05 ($p = 0.0363$), while the effect of silica fume content (B) and liquid-solid ratio (C) does not reach the significance level within the investigation scope of this study ($p = 0.7019$ and 0.2051). The results of range analysis were consistent with the results of variance analysis. The order of factors affecting fluidity was A ($R = 15.00$) > C ($R = 6.33$)>B ($R = 2.00$). According to the trend of average values, the average values of A from A1 to A3 are 117.33, 131.67 and 132.33 respectively, showing a monotonic increasing trend; the average values of C from C1 to C3 are 124.33, 126.33 and 130.67 respectively, also showing an increasing trend; and the average values of B from B1 to B3 are 128.33, 126.67 and 126.33 respectively, showing a slight decreasing trend overall. According to the analysis, the optimum combination is A3B1C3 (modulus

10.3389/fmats.2026.1759190

TABLE 5 Polar deviation calculation results.

Evaluation index	Statistical parameter	Factor A	Factor B	Factor C	Optimal combination
3d compressive strength (MPa)	k1	19.73	21.70	28.73	A2B1C1
	k2	27.90	16.10	20.80	
	k3	11.73	21.57	9.83	
	R	16.17	5.60	18.90	
	Sum of squares	392.06	61.26	540.42	
	p	0.0244	0.1381	0.0178	
7d compressive strength (MPa)	k1	27.8	29.77	44.00	A2B1C1
	k2	34.4	24.03	27.80	
	k3	20.43	28.83	10.83	
	R	13.97	5.73	33.17	
	Sum of squares	292.90	56.78	1,650.34	
	p	0.0394	0.1746	0.0072	
28d compressive strength (MPa)	k1	33.87	34.03	49.93	A2B1C1
	k2	37.30	29.33	32.83	
	k3	24.70	32.50	13.10	
	R	12.60	4.70	36.83	
	Sum of squares	254.58	34.47	2038.51	
	p	0.0410	0.2401	0.0053	
Fluidity(mm)	k1	117.33	128.33	124.33	A3B1C3
	k2	131.67	126.67	126.33	
	k3	132.33	126.33	130.67	
	R	15.00	2.00	6.33	
	Sum of squares	430.89	6.89	62.89	
	p	0.0363	0.7019	0.2051	

1.0, silica fume 15%, liquid-solid ratio 0.95) for highest working performance.

It should be noted that when the strength and fluidity are optimized simultaneously, the optimal levels of A and C are not consistent. The silicate modulus influences the solution viscosity and polymerization behavior by regulating the SiO_2/Na_2O ratio. When the modulus is too low and the alkalinity is excessively high, the solution exhibits high viscosity, which hinders the polycondensation process. If the modulus is too high, the reaction rate will be insufficient. Moderate modulus is more conducive to balancing mechanical properties and workability.

Moreover, reducing the liquid-to-solid ratio increases reactant concentration and matrix compactness, improving strength but reducing fluidity due to limited free water. In contrast, increasing this ratio enhances workability but weakens strength because of dilution and higher porosity (Albidah et al., 2021; Luan et al., 2021). And optimization of activator modulus together with water content is critical for achieving balanced mechanical and rheological performance (Park et al., 2022). Based on these findings and the results summarized in Table 4, a silicate modulus of 0.9, silica fume content of 15%, and liquid to solid ratio of 0.75 were selected as the reference mix for subsequent additive performance evaluation.

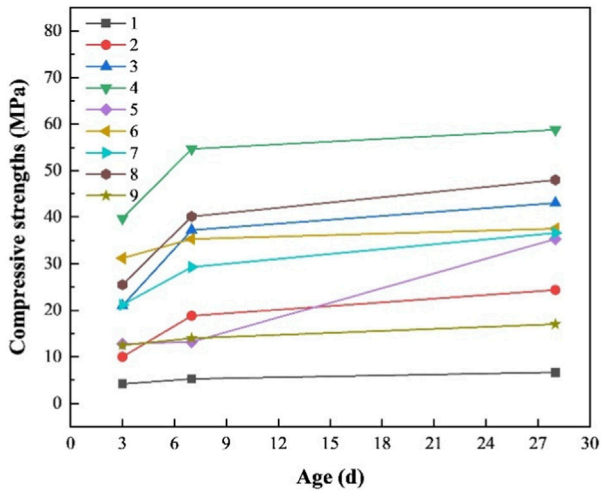

FIGURE 2
Compressive strength of geopolymer at different curing ages.

3.2 Effect of superplasticizer on the performance of geopolymer

3.2.1 Effect of superplasticizer on initial fluidity of fresh slurry

The analysis in this subsection focuses on establishing how different superplasticizers modify the initial workability of metakaolin-based geopolymer pastes. According to the strength test results, the dosage of sodium lignosulfonate, naphthalene-based additives and melamine are 0.5%, 1%, 1.5%, respectively. The dosages of polycarboxylic acid additives are 0.1%, 0.4%, 0.7%, respectively, and the silane coupling agent KH550 are 0.2 mL, 0.5 mL, 0.8 mL, 1.1 mL, respectively. The results of fluidity test are shown in Figure 3. The initial fluidity of the metakaolin-based polymer without superplasticizer is 122 mm.

As shown in Figure 3, the improvement effect of various superplasticizers on the fluidity of metakaolin based polymer is as follows: sodium lignosulfonate > silane coupling agent > melamine > polycarboxylic acid > naphthalene series superplasticizer. Sodium lignosulfonate and silane coupling agents initially increased and then decreased with the increase of dosage. Specifically, when 0.5% sodium lignosulfonate was added, the fluidity of slurry increased to 127 mm; when the addition amount increased to 1.0%, the initial fluidity further increased to 130 mm, which was about 7% higher than that of the reference. When the dosage continued to increase to 1.5%, the fluidity decreased slightly. The optimal dosage of silane coupling agent was about 0.8 mL, and the fluidity improvement effect was similar to that of sodium lignosulfonate. In contrast, melamine, naphthalene series and polycarboxylic acid superplasticizer had negative effects overall. At a dosage of 0.5%, melamine achieved an initial flowability of 125 mm, which was slightly higher than that of the control group. However, its effect was noticeably weaker than that of sodium lignosulfonate. When the dosage increased to 1.5%, the flowability decreased to 118 mm. The naphthalene-based superplasticizer yielded an initial flowability of only 115 mm at 0.5% dosage, representing a 5.7% decrease compared with the reference, and further decreased to 107 mm at 1.5% dosage, a reduction of 12.3%. The polycarboxylate superplasticizer exhibited a similar trend: at a dosage of 0.7%, the flowability dropped to 112 mm, 8.2% lower than that of the reference. This may be attributable to the poor compatibility of melamine with highly alkaline systems, while naphthalene-based and polycarboxylate superplasticizers tend to adsorb or complex with reactive silicate ions in the metakaolin–sodium silicate system, weakening their dispersing effect (Derkani et al., 2022). This interaction promotes early structural flocculation of the paste, thereby suppressing flowability.

3.2.2 Effect of superplasticizer on bleeding volume of slurry

To further evaluate the time-dependent workability performance, this subsection examines the evolution of flowability loss under various superplasticizers. The bleeding volume of geopolymer slurry with five different superplasticizers at high and low superplasticizers is shown in Figure 4. Without superplasticizer, the bleeding volume of metakaolin geopolymer in 120 min is 2.5 mL ~3 mL.

As shown in Figure 4, at high dosage, the five kinds of superplasticizer did not effectively inhibit slurry bleeding. Polycarboxylic acid additive had the largest bleeding volume, with bleeding volume of 8 mL at 120 min, followed by sodium lignosulfonate. This phenomenon can be attributed to the competitive adsorption of superplasticizer molecules on particle surfaces and in the solution at high dosages, resulting in the saturation of effective dispersion sites (Zhang et al., 2021; Partschefeld et al., 2023). Consequently, the electrostatic repulsion and steric hindrance effects are weakened, which in turn accelerated particle reaggregation and water bleeding (Plank and Winter 2008).

In contrast, at lower content, except polycarboxylic acid, other superplasticizers showed certain improvement effect. At 120 min, the bleeding volumes of melamine, sodium lignosulfonate, naphthalene series superplasticizer, polycarboxylic acid and KH550 silane coupling agent were 2.3 mL, 1.9 mL, 2.4 mL, 5.0 mL and 2.0 mL respectively. Sodium lignosulfonate > KH550 > melamine > naphthalene series superplasticizer > polycarboxylic acid, which was basically consistent with the results of fluidity test, further indicating the advantages of sodium lignosulfonate and KH550 in improving the working performance of geopolymer.

The test results show that the high effective superplasticizer commonly used in cement system can improve the fluidity of metakaolin based polymer. In contrast, sodium lignosulfonate and KH550 showed better dispersion and water reduction effects, but the dosage should be strictly controlled to avoid the negative effects caused by excessive addition, among which the optimum dosage of sodium lignosulfonate was 1.0%, and the optimum dosage of silane coupling agent KH550 was 0.8 mL/150g.

3.3 Physical stability

3.3.1 Stability performance

This subsection investigates the bleeding behavior and physical stability of the geopolymer slurry to further clarify the influence of superplasticizers on mixture uniformity. Figure 5 shows the

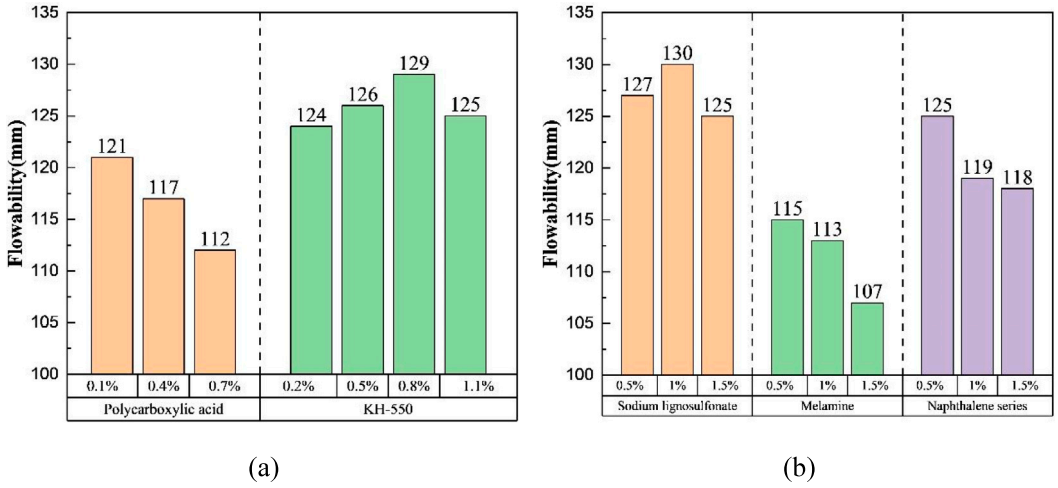

FIGURE 3
Initial fluidity of slurry with five superplasticizers at different dosages **(a)** Polycarboxylic and KH-550, **(b)** Sodium lignosulfonate, melamine and naphthalene series.

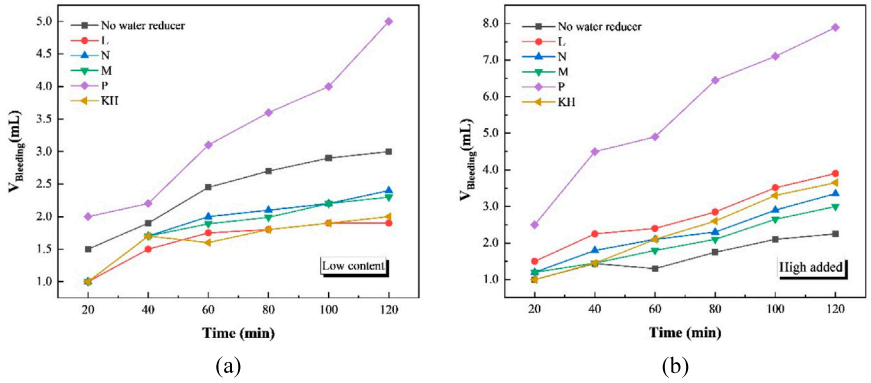

FIGURE 4
Bleeding volume of slurry with different superplasticizers: **(a)** Low superplasticizer; **(b)** High superplasticizer.

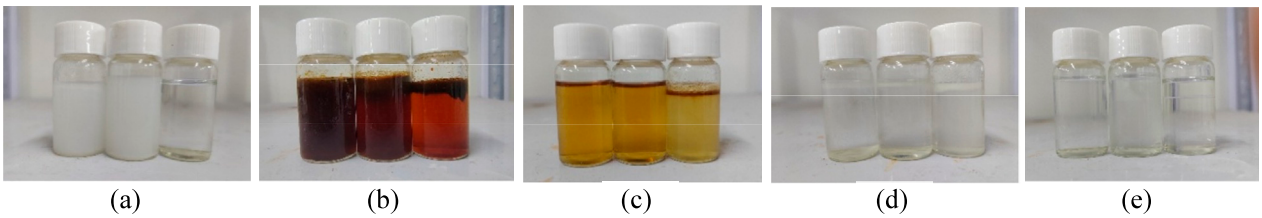

FIGURE 5
Morphological characteristics of superplasticizers in sodium silicate solution **(a)** M, **(b)** L, **(c)** N, **(d)** P, **(e)** KH.

appearance characteristics of superplasticizers in sodium silicate solutions. The silicate modulus from left to right in the figure is 0.8, 1.4 and 2.0 respectively.

The results showed that the lower the modulus of sodium silicate, the worse the solubility and the more unstable the appearance of the system. When the modulus is 2.0, all the systems were clear and homogeneous except for polycarboxylic acid superplasticizer. When the modulus is 0.8, precipitation or stratification occurred in all five superplasticizers. Under the conditions of this study, the appearance stability from high to low is sodium lignosulfonate, naphthalene series water reducer > KH550 silane coupling agent, melamine > polycarboxylic acid

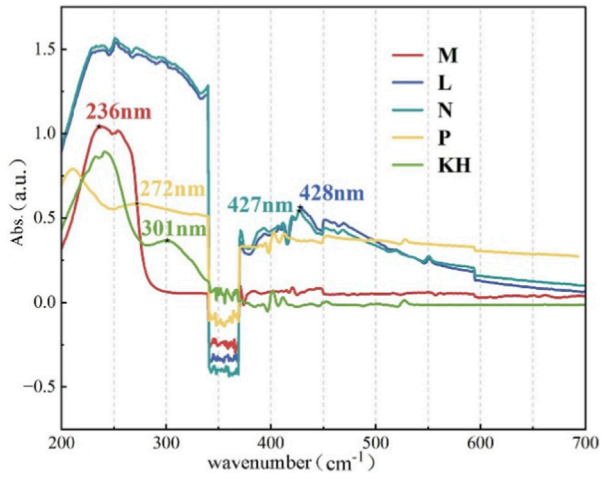

FIGURE 6
Absorbance curves of various superplasticizers.

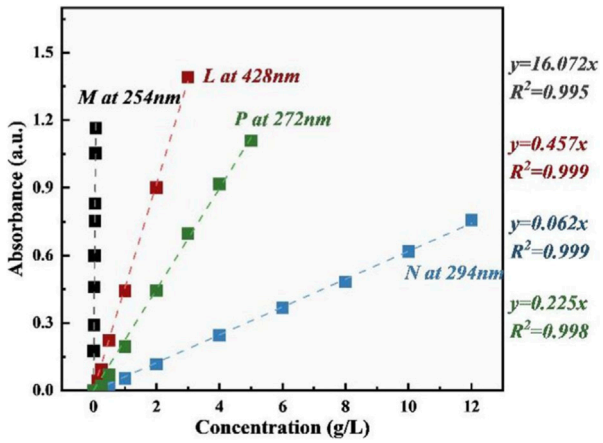

FIGURE 7
Absorbance-Concentration standard curves.

superplasticizer (Luukkonen et al., 2018; Ren et al., 2023). This result highlights the adaptation advantage of lignin superplasticizer in strong alkali silicate environment.

3.3.2 Solubility

The absorbance curves of the superplasticizer are shown in Figure 6, and the absorbance-concentration calibration fitting curves of the superplasticizer are shown in Figure 7.

Except KH55, the other superplasticizer have good linearity at their respective characteristic wavelengths ($R^2 \geq 0.995$). The continuous hydrolysis-polycondensation of KH550 in water leads to the spectrum drifting with time, and it is challenging to obtain the steady-state concentration-absorbance relationship.

Table 6 shows the incompatibility rate of each additive in different modulus sodium silicate solutions. As shown in Table 6, with the decrease of silicate modulus (Ms), the insolubility of each additive increased, indicating that the solubility of the system

TABLE 6 Insolubility of four superplasticizer.

Water reducer	Sodium silicate modulus	Theoretical concentration C_0 = 12.5 g/L	
		C' (g/L)	η (%)
M	0.8	0.283749	97.73
	1.4	0.742537	94.06
L	0.8	3.941251	68.47
	1.4	7.040273	43.68
N	0.8	1.837504	85.3
	1.4	10.55125	15.59
P	0.8	0.980285	92.16
	1.4	2.691247	78.47

decreased and the appearance stability deteriorated. Melamine had an insolubility of 94.06% and 97.73% when the silicate modulus was 1.4 and 0.8, respectively, indicating that its solubility was extremely low, making it difficult to reduce water content. Sodium lignosulfonate still maintains a certain solubility at low modulus (e.g., the insolubility was significantly lower than other superplasticizers when Ms = 0.8), which was consistent with its better workability than the same kind. Naphthalene superplasticizers were highly sensitive to modulus, rising sharply from 15.59% of Ms = 1.4 to 85.30% of Ms = 0.8, indicating that they are more suitable for medium and high modulus conditions. The solubility of polycarboxylic acid superplasticizer was poor, and the insolubility reached 78.47% and 92.16% respectively when Ms = 1.4 and 0.8. In general, the decrease of modulus was accompanied by the increase of ionic strength and pH, which easily initiated stratification and competitive adsorption, thus inhibiting the effective dissolution and dispersion of superplasticizer, while sodium lignosulfonate showed relatively better adaptability in this strong alkali silicate environment.

3.4 Effect of sodium ligninsulfonate and silane coupling agent on fluidity loss of freshly mixed slurry over time

It can be seen from Subsection 3.2 that sodium lignosulfonate and silane coupling agent have the best effect on improving the working performance of metakaolin based polymer under appropriate dosage. Select the dosage with the best water reduction effect (sodium lignosulfonate 1.0%, KH550 silane coupling agent 0.8 mL/150g powder) and observe the fluidity loss of polymer slurry in 60 min, and the results are shown in Figure 8.

As can be seen from Figure 8 that compared with the reference, both superplasticizers improved the initial fluidity of the slurry: sodium lignosulfonate increased by 7.6%, KH550 increased by 6.8%. When the time was prolonged to 30 min, the fluidity of blank

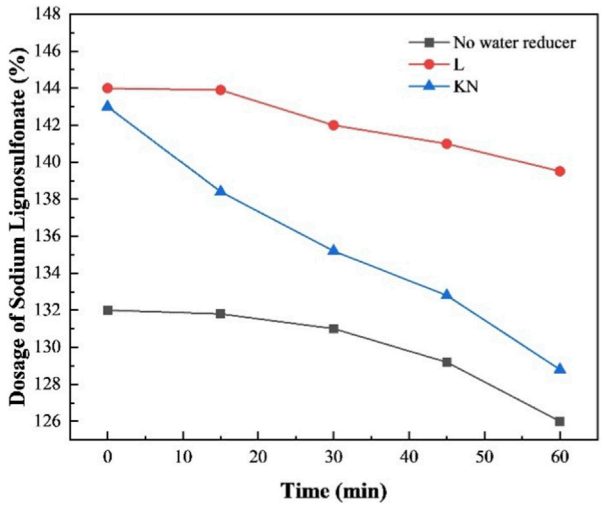

FIGURE 8
Loss of slurry fluidity with time.

group, lignin group and KH550 group was 131 mm, 140 mm and 134 mm respectively, and lignin group and KH550 group increased by 6.9% and 2.3% respectively compared with the reference. At 60 min, the fluidities of the three groups were 126 mm, 137 mm and 128 mm, respectively, and the increase ranges were 8.7% and 1.6%, respectively. The lignin group was significantly higher than the reference from 0 to 60 min, showing better fluidity retention; while the KH550 group decreased rapidly with time, and the gap with the reference gradually narrowed, and it was close to the reference at 60 min.

From the mechanism point of view, the early dissolution-polycondensation process of geopolymer is parallel: silicon and aluminum in metakaolin dissolve out and promote particle dispersion at the initial stage, and the viscosity of the system changes little or decreases temporarily; with the reaction advancing, Si-O-Al three dimensional network is gradually established, yield stress and viscosity increase, and fluidity decreases accordingly (Romagnoli et al., 2012; Rodrigue Kaze et al., 2021). KH550 was hydrolyzed and condensed with hydroxyl groups on the surface to form silicon-oxygen bonds, which could enhance the bonding of particle-matrix interface and accelerate the structuring, thus causing faster fluidity loss (Yu et al., 2024). On the contrary, Na-LS formed a charged adsorption layer on the particle surface, which provided electrostatic repulsion and certain dispersion stability, so it showed better fluidity retention. In conclusion, sodium lignosulfonate was selected in the subsequent experiments to further evaluate its effect on the mechanical properties of geopolymers (Kalina et al., 2022; Ren et al., 2023).

3.5 Effect of sodium lignosulfonate on mechanical properties of geopolymer with different content

The influence of lignin on compressive strength of geopolymer at 0%, 0.5%, 1% and 1.5% is shown in Table 7.

TABLE 7 Effect of lignin content on compressive strength of geopolymer.

Dosage	Age		
	3d	7d	28d
0	22.8	38.4	46.1
0.5%	22.5	37.9	45.3
1%	21.0	36.4	45.0
1.5%	19.9	35.9	44.1

It can be seen from Table 7 that sodium lignosulfonate (Na-LS) has a small adverse effect on the compressive strength of geopolymer, and it shows a decreasing trend with the increase of dosage. When the dosage increased to 1.5%, the 3-day, 7-day, and 28-day strength decreased from 22.8 MPa to 19.9 MPa, from 38.4 MPa to 35.9 MPa, and from 46.1 MPa to 44.1 MPa, corresponding to reductions of 12.7%, 6.5%, and 4.3%, respectively, with the overall magnitude of reduction being relatively limited. This behavior may be attributed to the admixture's reduced stability in highly alkaline media, which may slightly weaken particle dispersion and hinder gel densification (Palacios and Puertas, 2005). In conjunction with the results on workability presented in Subsection 3.3, Na-LS demonstrated a significant effect in enhancing flowability, while its negative impact on strength remains relatively controllable. Considering the working performance and strength loss, the recommended sodium lignosulfonate content is 1.0%.

3.6 Analysis of action mechanism of superplasticizer

3.6.1 Fourier transform infrared spectroscopy

FTIR spectroscopy is employed to identify molecular-level interactions between the admixtures and the geopolymer network, providing insight into their chemical action mechanisms. Figure 9 illustrated the FTIR comparison of various water reducing agents in different modulus sodium silicate solutions.

L, N, P can be seen in water with their respective hydrophobic and hydrophilic fragments: aromatic (C=C/C-C) skeleton at around 1,600/1,510 cm^{-1}, C-N/C-O vibration at around 1,186 cm^{-1}, -CH/-CH stretching at around 2,881 cm^{-1}, and sulfonate characteristics (S=O at around 1,358 cm^{-1}, S-O at around 1,032 cm^{-1}), amino (N-H at around 3,469 cm^{-1} and 3,416 cm^{-1}), and polyether segments (C-O-C at around 1,097 cm^{-1}). Upon exposure to sodium silicate, these peaks exhibited attenuation and slight shifts, signifying hydrolysis and ionic shielding effects under strongly alkaline and high-ionic-strength conditions. On one hand, labile bonds (e.g., ether or amide) underwent partial cleavage, resulting in reduced molecular weight and disrupted continuity of hydrophobic segments (Partschefeld et al., 2023). On the other hand, competitive adsorption of silicate species at polar sites impaired surface activation and dispersion efficacy, thereby corroborating the observed decline in workability (Ren et al., 2023).

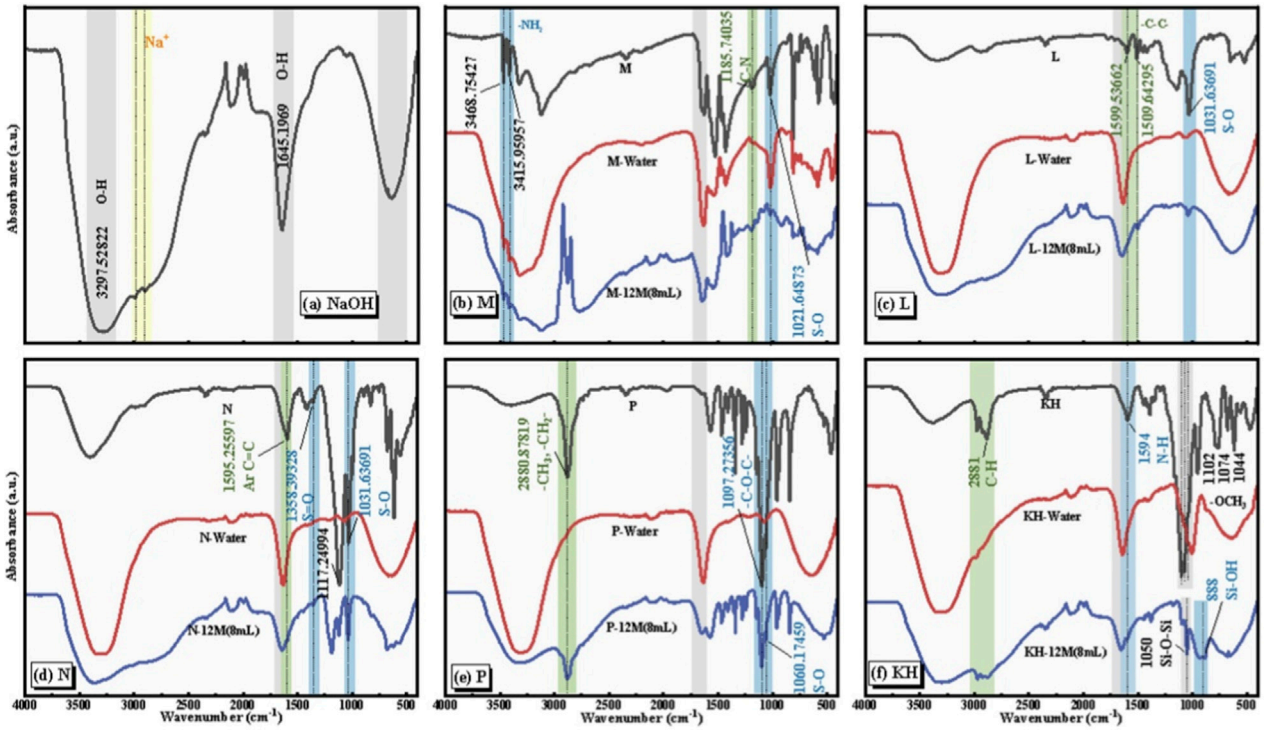

FIGURE 9
FTIR spectra of superplasticizers **(a)** NaOH, **(b)** M, **(c)** L, **(d)** N, **(e)** P, **(f)** KH.

The change of KH system was more typical: the signs of methoxy group to silanol (Si-OH) conversion (3,200–3,500 cm^{-1} wide peak enhancement, 1,000–1,100 cm^{-1} wide region Si-O-Si signal enhancement) indicate that silane hydrolysis-condensation occurs in sodium silicate, and Si-O-Si, Si-O-Al bonds were formed with the matrix (Issa and Luyt, 2019). Meanwhile, the change of C-H intensity indicates that the organic end groups were rearranged or partially broken. The interfacial reaction was beneficial to early network construction, but also shortened the machinable time, which was consistent with the result of low fluidity retention of KH group. Overall, KH-550 accelerates early network formation but leads to rapid loss of flowability, which accounts for its poor suitability for enhancing slurry workability.

3.6.2 Surface tension effects

This subsection assesses how each superplasticizer alters the surface tension of the system to clarify whether surface activity contributes to its water-reducing behavior. Select the sodium silicate solution with modulus of 0.9 to test the effect of additive type on the surface tension. The results are shown in Figure 10.

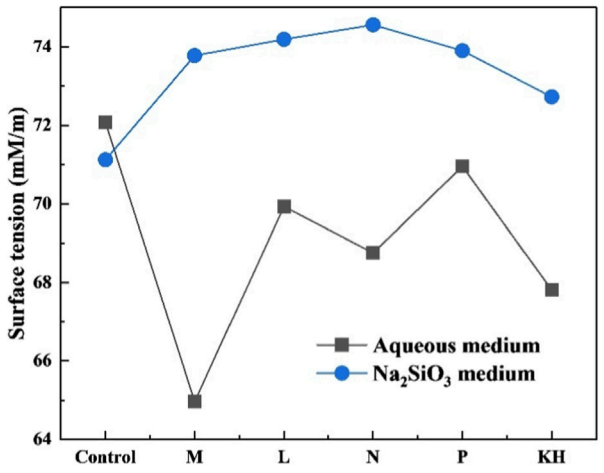

FIGURE 10
Surface tension of sodium silicate solutions with different superplasticizers.

It can be seen from Figure 10 that the addition of superplasticizer reduced the surface tension of aqueous solution, among which melamine has the most significant effect, and the surface tension of aqueous solution decreases from about 72 mM/m to 65 mM/m (9.7% decrease). Sodium lignosulfonate, naphthalene series superplasticizer, polycarboxylic acids and KH550 also decreased by varying degrees. On the contrary, in sodium silicate medium, except KH550, the surface tension of other systems was higher than that of sodium silicate body (about 71 $mN{\cdot}m^{-1}$). Moreover, the surface tension of the same superplasticizer in sodium silicate solution was significantly higher than its value in aqueous solution. These observations suggest that the improved fluidity of metakaolin-based geopolymers is not governed by surface-tension reduction, but is instead primarily driven by particle dispersion, electrostatic repulsion, and interfacial chemical interactions (Fan et al., 2023; da Silva et al., 2026). This behavior contrasts with that reported for

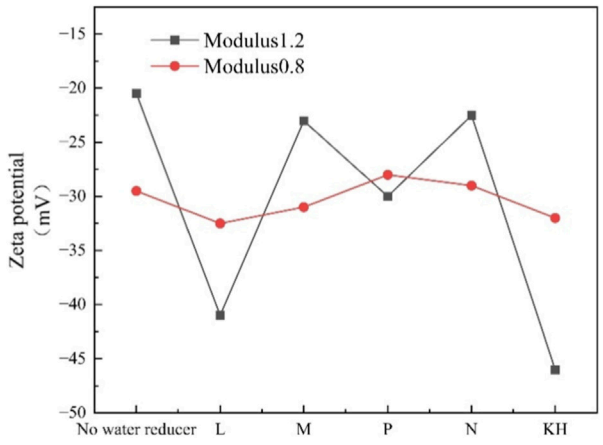

FIGURE 11
Zeta potential of the system incorporating different superplasticizers.

cementitious systems (Lu et al., 2021), where surface activity plays a more prominent role, further confirming that surface tension is not the controlling mechanism for workability in alkaline geopolymer environments.

3.6.3 Zeta potential

Zeta potential (ZP) represents the electrokinetic potential at the shear plane of suspended particles, indicating their surface charge and electrostatic interactions. A higher absolute ZP implies stronger repulsive forces between particles, leading to improved dispersion stability and enhanced slurry workabilit. The ZP of metakaolin-based polymer slurries with different superplasticizers are shown in Figure 11.

It can be seen from Figure 11 that, under a silicate modulus of 1.2, all superplasticizers significantly increase the absolute ZP of metakaolin particles, thereby enhancing electrostatic repulsion. The differences among the admixtures are evident. Sodium lignosulfonate and the KH-550 silane coupling agent show the largest increases in absolute ZP, rising from approximately 21 mV to about 40 mV and 45 mV, respectively. This notable increase aligns well with the observed improvement in slurry workability. Polycarboxylic acid also exerts a moderate effect, increasing the absolute ZP to around 30 mV. In contrast, when the silicate modulus is 0.8, the enhancement of electrostatic repulsion is generally weaker. Under this condition, sodium lignosulfonate and KH550 perform slightly better than melamine, whereas polycarboxylic-acid- and naphthalene-based superplasticizers have the weakest effect, with absolute ZP values even lower than that of the blank sample. This trend is consistent with the results of the macroscopic fluidity tests.

Consistent with the FTIR and surface-tension analyses, the zeta-potential results further confirm that changes in alkalinity significantly influence interparticle interactions in metakaolin-based geopolymers. When the silicate modulus decreases from 1.2 to 0.8, the absolute ZP of the blank sample increases from approximately 21 mV–30 mV, indicating that particle surface charging and electrostatic repulsion are enhanced with increasing alkalinity. In contrast, sodium lignosulfonate and KH550 exhibit a notable decrease in absolute ZP (about 20%), suggesting that their dispersion efficiency is suppressed under more alkaline conditions. The variation in polycarboxylic acid is relatively small, implying that it is less sensitive to modulus changes, whereas the slight increase observed for naphthalene- and melamine-based superplasticizers is mainly attributed to the intensified ionization of the sodium silicate matrix at lower modulus.

As the silicate modulus decreases, the electrostatic activity of the alkaline solution increases, but the resulting dispersion behavior varies markedly among different superplasticizers. KH-550 and sodium lignosulfonate show pronounced attenuation in dispersion performance due to electrostatic shielding under high alkalinity and elevated ionic strength, indicating that their effectiveness may be compromised in on-site geopolymer mixtures with strong alkaline activators. In contrast, polycarboxylic acid maintains relatively stable dispersion behavior, while naphthalene- and melamine-based superplasticizers exhibit only limited responsiveness to changes in modulus. These differentiated responses highlight the importance of selecting alkali-tolerant superplasticizers to ensure reliable workability in practical metakaolin-based geopolymer construction, particularly when activator modulus fluctuates during field mixing.

4 Conclusion

In this study, the mix proportions of metakaolin-based alkali-activated geopolymers were optimized through orthogonal experimental design, and the performance and mechanisms of five representative superplasticizers were systematically evaluated. The main conclusions are as follows:

1. The optimal mixture was obtained at a silicate modulus of 0.9, a liquid-to-solid ratio of 0.75, and a silica fume content of 15%. Under these conditions, the compressive strengths at 3, 7, and 28 days were 39.7 MPa, 54.7 MPa, and 58.8 MPa, respectively, and the fluidity reached 132 mm.
2. Sodium lignosulfonate and KH-550 exhibited stronger water-reducing effects than the other superplasticizers. However, KH-550 markedly accelerated early polymerization, leading to rapid loss of flowability over time. Although lignosulfonate caused a slight reduction in compressive strength, the impact was limited, and an optimal dosage of 1.0% was determined.
3. The mechanistic findings reveal that the water-reducing behavior of superplasticizers in metakaolin-based geopolymers is fundamentally different from that reported in Portland-cement systems. The improvement in flowability is not governed by surface-tension reduction, but rather by interfacial chemical interactions and structure-dependent electrostatic dispersion. At high silicate modulus, all superplasticizers enhance zeta potential and electrostatic repulsion, whereas at low modulus, only lignosulfonate and KH-550 maintain effective dispersion owing to their stronger interfacial activity or ionization behavior. These results clarify the molecular-level dispersion mechanisms in highly alkaline geopolymer environments and provide new insights distinct from existing studies.

Overall, this study elucidates how molecular structure and alkaline tolerance govern the dispersion behavior of superplasticizers, thereby providing a mechanistic basis for the

formulation of workability-enhancing admixtures for metakaolin-based geopolymers. Future work should focus on clarifying the degradation pathways of admixtures under highly alkaline conditions and on developing alkali-resistant superplasticizer systems better aligned with geopolymer chemistry.

Data availability statement

The original contributions presented in the study are included in the article/supplementary material, further inquiries can be directed to the corresponding author.

Author contributions

GZ: Formal Analysis, Methodology, Data curation, Conceptualization, Writing – original draft, Investigation. FC: Methodology, Writing – original draft, Validation. TL: Data curation, Investigation, Visualization, Writing – original draft. CS: Formal Analysis, Validation, Writing – review and editing. LY: Writing – review and editing, Investigation, Data curation, Visualization. YC: Formal Analysis, Visualization, Writing – review and editing, Software. WS: Methodology, Project administration, Writing – review and editing, Resources. HC: Writing – review and editing. WG: Validation, Writing – review and editing. RW: Supervision, Writing – review and editing. BM: Project administration, Conceptualization, Funding acquisition, Writing – review and editing, Supervision.

Funding

The author(s) declared that financial support was received for this work and/or its publication. This research was funded by the CCCC-SHEC Seventh Highway Engineering Co., Ltd under the grant number of 220221230584, 220221230594 and 220221230552. The funder was not involved in the study design, collection, analysis, interpretation of data, the writing of this article, or the decision to submit it for publication.

Conflict of interest

Authors GZ, FC, TL, and CS were employed by The 7th Engineering Co., Ltd. of CCCC Second Highway Engineering Bureau.

The remaining author(s) declared that this work was conducted in the absence of any commercial or financial relationships that could be construed as a potential conflict of interest.

Generative AI statement

The author(s) declared that generative AI was not used in the creation of this manuscript.

Any alternative text (alt text) provided alongside figures in this article has been generated by Frontiers with the support of artificial intelligence and reasonable efforts have been made to ensure accuracy, including review by the authors wherever possible. If you identify any issues, please contact us.

Publisher's note

References

Albidah, A., Alghannam, M., Abbas, H., Almusallam, T., and Al-Salloum, Y. (2021). Characteristics of metakaolin-based geopolymer concrete for different mix design parameters. *J. Mater. Res. Technol.* 10, 84–98. doi:10.1016/j.jmrt.2020.11.104

Asghar, R., Khan, M. A., Alyousef, R., Javed, M. F., and Ali, M. (2023). Promoting the green construction: scientometric review on the mechanical and structural performance of geopolymer concrete. *Constr. Build. Mater.* 368, 130502. doi:10.1016/j.conbuildmat.2023.130502

Aupoil, J., Champenois, J. B., De Lacaillerie, J. B. D., and Poulesquen, A. (2019). Interplay between silicate and hydroxide ions during geopolymerization. *Cem. Concr. Res.* 115, 426–432. doi:10.1016/j.cemconres.2018.09.012

Aziz, I. H., Abdullah, M. M. A., Heah, C. Y., and Liew, Y. M. (2020). Behaviour changes of ground granulated blast furnace slag geopolymers at high temperature. *Adv. Cem. Res.* 32, 465–475. doi:10.1680/jadcr.18.00162

Da Silva, M. R. C., De Castro Carvalho, I., Silvestro, L., Lei, L., Kirchheim, A. P., and Walkley, B. (2026). Advances in understanding the mechanisms of particle dispersion and performance of superplasticisers in alkali-activated materials – a systematic literature review. *Cem. Concr. Compos.* 166, 106360. doi:10.1016/j.cemconcomp.2025.106360

Derkani, M. H., Bartlett, N. J., Koma, G., Carter, L. A., Geddes, D. A., Provis, J. L., et al. (2022). Mechanisms of dispersion of metakaolin particles *via* adsorption of sodium naphthalene sulfonate formaldehyde polymer. *J. Colloid Interface Sci.* 628, 745–757. doi:10.1016/j.jcis.2022.07.166

Fan, Z., Kong, L., Lu, J., and Wang, X. (2023). Mechanism study of effect of superplasticizers on the fluidity of alkali-activated materials. *Mater. Struct.* 56, 29. doi:10.1617/s11527-023-02120-0

Gao, K., Lin, K.-L., Wang, D., Hwang, C.-L., Shiu, H.-S., Chang, Y.-M., et al. (2014). Effects SiO2/Na2O molar ratio on mechanical properties and the microstructure of nano-SiO2 metakaolin-based geopolymers. *Constr. Build. Mater.* 53, 503–510. doi:10.1016/j.conbuildmat.2013.12.003

Ge, X. A., Hu, X., and Shi, C. J. (2022). The effect of different types of class F fly ashes on the mechanical properties of geopolymers cured at ambient environment. *Cem. and Concr. Compos.* 130, 104528. doi:10.1016/j.cemconcomp.2022.104528

Hattaf, R., Aboulayt, A., Samdi, A., Lahlou, N., Touhami, M. O., Gomina, M., et al. (2021). Metakaolin and fly ash-based matrices for geopolymer materials: setting kinetics and compressive strength. *Silicon* 14, 6993–7004. doi:10.1007/s12633-021-01447-z

Hu, Y., Wang, H., Zhou, L., and Airey, G. D. (2024). "Towards an enhanced understanding of the functional groups within bitumen during ageing processes," in *Advances in functional pavements*. London: CRC Press.

Hu, Y., Cheng, X., Sreeram, A., Si, W., Li, B., Pipintakos, G., et al. (2025a). Enhancing fatigue resistance and low-temperature performance of asphalt pavements using antioxidant additives. *Mater. Struct.* 58, 46. doi:10.1617/s11527-025-02574-4

Hu, Y., Yin, Y., Sreeram, A., Liu, J., Si, W., Tang, D., et al. (2025b). Nano-aggregation of asphaltenes and its influence on the multiscale properties of bitumen

recycled through multiple ageing and rejuvenation cycles. *Chem. Eng. J.* 512, 162348. doi:10.1016/j.cej.2025.162348

Hu, Y., Yin, Y., Sreeram, A., Si, W., Airey, G. D., Li, B., et al. (2025c). Atomic force microscopy (AFM) based microstructural and micromechanical analysis of bitumen during ageing and rejuvenation. *Constr. Build. Mater.* 467, 140387. doi:10.1016/j.conbuildmat.2025.140387

Huang, W., and Wang, H. (2024). Formulation development of metakaolin geopolymer with good workability for strength improvement and shrinkage reduction. *J. Clean. Prod.* 434, 140431. doi:10.1016/j.jclepro.2023.140431

Issa, A. A., and Luyt, A. S. (2019). Kinetics of alkoxysilanes and organoalkoxysilanes polymerization: a review. *Polym. (Basel)* 11. doi:10.3390/polym11030537

Johnson, A. T., Sosa, D., Arredondo, R., Li, H. W., Yuan, Z. S., and Xu, C. B. (2023). Production of bio-based concrete water reducers from renewable resources: a review. *Biofuels Bioprod. and Biorefining-Biofpr* 17, 1425–1444. doi:10.1002/bbb.2501

Kalina, L., Bílek, V., Hrubý, P., Iliushchenko, V., Kalina, M., and Smilek, J. (2022). On the action mechanism of lignosulfonate plasticizer in alkali-activated slag-based system. *Cem. Concr. Res.* 157. doi:10.1016/j.cemconres.2022.106822

Keskin-Topan, Y., Bessaies-Bey, H., Petit, L., Tran, N.-C., D'espinose De Lacaillerie, J.-B., Rossignol, S., et al. (2024). Effect of maximum packing fraction of powders on the rheology of metakaolin-based geopolymer pastes. *Cem. Concr. Res.* 179, 107482. doi:10.1016/j.cemconres.2024.107482

Kou, S.-C., Poon, C.-S., Agrela, F. J. C., and Composites, C. (2011). *Comparisons of natural and recycled aggregate concretes prepared with the addition of different mineral admixtures*, 33, 788–795.

Li, N., Shi, C. J., Zhang, Z. H., Zhu, D. J., Hwang, H. J., Zhu, Y. H., et al. (2018). A mixture proportioning method for the development of performance-based alkali-activated slag-based concrete. *Cem. and Concr. Compos.* 93, 163–174. doi:10.1016/j.cemconcomp.2018.07.009

Li, B., Zhao, H., Zhou, J., Yao, T., Guo, F., and Hu, Y. (2024). Investigation on sound absorption coefficients of porous asphalt concrete under different clogging conditions. *Constr. Build. Mater.* 428, 136081. doi:10.1016/j.conbuildmat.2024.136081

Li, B., Zhang, Y., Wei, D., Yao, T., Hu, Y., and Dou, H. (2025). Evolution of clogging of porous asphalt concrete in the seepage process through integration of computer tomography, computational fluid dynamics, and discrete element method. *Computer-Aided Civ. Infrastructure Eng.* 40, 1652–1674. doi:10.1111/mice.13419

Liu, X., Lu, M. Y., Sheng, K., Shao, Z. W., Yao, Y. L., and Hong, B. N. (2023). Development of new material for geopolymer lightweight cellular concrete and its cementing mechanism. *Constr. Build. Mater.* 367, 130253. doi:10.1016/j.conbuildmat.2022.130253

Lu, C. F., Zhang, Z. H., Shi, C. J., Li, N., Jiao, D. W., and Yuan, Q. (2021). Rheology of alkali-activated materials: a review. *Cem. and Concr. Compos.* 121, 104061. doi:10.1016/j.cemconcomp.2021.104061

Luan, C., Shi, X., Zhang, K., Utashev, N., Yang, F., Dai, J., et al. (2021). A mix design method of fly ash geopolymer concrete based on factors analysis. *Constr. Build. Mater.* 272, 121612. doi:10.1016/j.conbuildmat.2020.121612

Luukkonen, T., Abdollahnejad, Z., Yliniemi, J., Kinnunen, P., and Illikainen, M. (2018). One-part alkali-activated materials: a review. *Cem. Concr. Res.* 103, 21–34. doi:10.1016/j.cemconres.2017.10.001

Ma, B., Wei, K., Huang, X. F., Shi, W. S., Chen, S. S., Hu, Y. P., et al. (2020). Preparation and investigation of NiTi alloy phase-change heat storage asphalt mixture. *J. Mater. Civ. Eng.* 32, 04020250. doi:10.1061/(asce)mt.1943-5533.0003338

Nath, P., and Sarker, P. K. (2014). Effect of GGBFS on setting, workability and early strength properties of fly ash geopolymer concrete cured in ambient condition. *Constr. Build. Mater.* 66, 163–171. doi:10.1016/j.conbuildmat.2014.05.080

Palacios, M., and Puertas, F. (2005). Effect of superplasticizer and shrinkage-reducing admixtures on alkali-activated slag pastes and mortars. *Cem. Concrete Research* 35, 1358–1367. doi:10.1016/j.cemconres.2004.10.014

Park, S., Yu, J., Oh, J. E., and Pyo, S. (2022). Effect of silica fume on the volume expansion of metakaolin-based geopolymer considering the silicon-to-aluminum molar ratio. *Int. J. Concr. Struct. Mater.* 16, 20. doi:10.1186/s40069-022-00510-2

Partschefeld, S., Tutal, A., Halmanseder, T., Schneider, J., and Osburg, A. (2023). Investigations on stability of polycarboxylate superplasticizers in alkaline activators for geopolymer binders. *Mater. (Basel)* 16, 5369. doi:10.3390/ma16155369

Plank, J., and Winter, C. (2008). Competitive adsorption between superplasticizer and retarder molecules on mineral binder surface. *Cem. Concr. Res.* 38, 599–605. doi:10.1016/j.cemconres.2007.12.003

Rakngan, W., Williamson, T., Ferron, R. D., Sant, G., and Juenger, M. C. G. (2018). Controlling workability in alkali-activated class C fly ash. *Constr. Build. Mater.* 183, 226–233. doi:10.1016/j.conbuildmat.2018.06.174

Ren, J., Zhou, Q.-Z., Yang, C.-H., and Bai, Y. (2023). Performance and interaction of sodium silicate activated slag with lignosulfonate superplasticiser added at different mixing stages. *Cem. Concr. Compos.* 136, 104900. doi:10.1016/j.cemconcomp.2022.104900

Rodrigue Kaze, C., Adesina, A., Alomayri, T., Assaedi, H., Kamseu, E., Chinje Melo, U., et al. (2021). Characterization, reactivity and rheological behaviour of metakaolin and Meta-halloysite based geopolymer binders. *Clean. Mater.* 2, 100025. doi:10.1016/j.clema.2021.100025

Romagnoli, M., Leonelli, C., Kamse, E., and Lassinantti Gualtieri, M. (2012). Rheology of geopolymer by DOE approach. *Constr. Build. Mater.* 36, 251–258. doi:10.1016/j.conbuildmat.2012.04.122

Shi, C. J., Qu, B., and Provis, J. L. (2019). Recent progress in low-carbon binders. *Cem. Concr. Res.* 122, 227–250. doi:10.1016/j.cemconres.2019.05.009

Shi, K., Ma, F., Falchetto, A. C., Fu, Z., Yuan, D., Song, R., et al. (2025a). Comprehensive review on the composition, influence, and inhibition of asphalt fumes. *J. Traffic Transp. Eng. Engl. Ed.* 12, 926–964. doi:10.1016/j.jtte.2024.09.006

Shi, K., Ma, F., Fu, Z., Lou, B., Barbieri, D. M., Li, J., et al. (2025b). Comprehensive evaluation of sulfur content and curing duration effects on the rheological performance of sulfur-extended bitumen. *Fuel* 393, 134979. doi:10.1016/j.fuel.2025.134979

Si, W., Zhang, B., Zhang, X., Xia, W., Cheng, X., Luo, X., et al. (2024). Maximizing the circularity of asphalt pavements by improving the RAP content in recycled asphalt mixtures. *Constr. Build. Mater.* 438, 137316. doi:10.1016/j.conbuildmat.2024.137316

Si, W., Xia, M., Zhang, B., Danzeng, G. A., Wang, X., Hu, Y., et al. (2026). Study on the preparation and performance optimization of wear-resistant asphalt pavement composite functional material reflective cooling coatings. *Constr. Build. Mater.* 508, 145055. doi:10.1016/j.conbuildmat.2025.145055

Singh, B., Rahman, M. R., Paswan, R., and Bhattacharyya, S. K. (2016). Effect of activator concentration on the strength, ITZ and drying shrinkage of fly ash/slag geopolymer concrete. *Constr. Build. Mater.* 118, 171–179. doi:10.1016/j.conbuildmat.2016.05.008

Wang, X., Ma, B., Yu, M., Mao, W., and Si, W. (2025). Testing and modeling of incomplete phase change heat storage and release of epoxy resin/microcapsule composite phase change materials for asphalt pavement. *J. Energy Storage* 105, 114672. doi:10.1016/j.est.2024.114672

Ye, N., Yang, J., Liang, S., Hu, Y., Hu, J., Xiao, B., et al. (2016). *Synthesis and strength optimization of one-part geopolymer based on red mud*, 111, 317–325.

Yu, M., Li, J., Zhao, C., Tan, W., Li, X., and Chen, P. (2024). Enhancing the performance of alkali-activated slag using KH-550 as a multi-functional admixture. *Case Stud. Constr. Mater.* 21, e03434. doi:10.1016/j.cscm.2024.e03434

Zhang, Z., Feng, Q., Zhu, W., Lin, X., Chen, K., Yin, W., et al. (2021). Influence of sand-cement ratio and polycarboxylate superplasticizer on the basic properties of mortar based on water film thickness. *Mater. (Basel)* 14, 4850. doi:10.3390/ma14174850

Zhong, Q. Y., Nie, H., Xie, G. L., and Peng, H. (2023). Experimental study on the characteristics, rheological factors, and flowability of MK-GGBFS geopolymer slurry. *J. Build. Eng.* 76, 107300. doi:10.1016/j.jobe.2023.107300